

Magnitude Invariant Parametrizations Improve Hypernetwork Learning

Jose Javier Gonzalez Ortiz
MIT CSAIL
josejg@mit.edu

John Guttag
MIT CSAIL
gutttag@mit.edu

Adrian V. Dalca
MIT CSAIL & HMS, MGH
adalca@mit.edu

Abstract

Hypernetworks, neural networks that predict the parameters of another neural network, are powerful models that have been successfully used in diverse applications from image generation to multi-task learning. Unfortunately, existing hypernetworks are often challenging to train. Training typically converges far more slowly than for non-hypernetwork models, and the rate of convergence can be very sensitive to hyperparameter choices. In this work, we identify a fundamental and previously unidentified problem that contributes to the challenge of training hypernetworks: a magnitude proportionality between the inputs and outputs of the hypernetwork. We demonstrate both analytically and empirically that this can lead to unstable optimization, thereby slowing down convergence, and sometimes even preventing any learning. We present a simple solution to this problem using a revised hypernetwork formulation that we call Magnitude Invariant Parametrizations (MIP). We demonstrate the proposed solution on several hypernetwork tasks, where it consistently stabilizes training and achieves faster convergence. Furthermore, we perform a comprehensive ablation study including choices of activation function, normalization strategies, input dimensionality, and hypernetwork architecture; and find that MIP improves training in all scenarios. We provide easy-to-use code that can turn existing networks into MIP-based hypernetworks.

1. Introduction

Hypernetworks, neural networks that predict the parameters of another neural network, are increasingly important models in a wide range of applications such as Bayesian optimization [27, 39, 54], generative models [1, 10, 44, 61], amortized model learning [3, 11, 22, 38, 58], continual learning [12, 21, 57], multi-task learning [34, 49, 53], and meta-learning [6, 62, 63]. Despite their advantages and growing use, training hypernetworks is challenging. Compared to non-hypernetwork-based models, training existing hypernetworks is often unstable. At best this increases training time, and at worst can prevent training from converging at

all. This burden limits their adoption, negatively impacting many applications. Existing hypernetwork heuristics, like gradient clipping [15, 27], are insufficient in many instances, while existing techniques aimed at improving standard neural network training often fail when applied to hypernetworks.

This work addresses a cause of training instability. We identify and characterize a previously unidentified hypernetwork design problem and provide a straightforward solution to address it. We demonstrate analytically and empirically that the typical choices of architecture and parameter initialization in hypernetworks cause a proportionality relationship between the scale of the hypernetwork inputs and the scale of the parameter outputs (Fig. 1a). The resultant fluctuations in predicted parameter scale lead to large fluctuations in the scale of the gradients during optimization, resulting in unstable training and slow convergence. In some cases, this phenomenon even prevents any meaningful learning. To overcome this issue, we propose a straightforward revision to hypernetwork models: Magnitude Invariant Parametrizations (MIP). MIP effectively eliminates the influence of the scale of hypernetwork inputs on the scale of the predicted parameters, while retaining the representational power of existing formulations. We demonstrate the effectiveness of our proposed solution across several hypernetwork learning tasks, providing evidence that hypernetworks using MIP achieve faster convergence without compromising model accuracy (Fig. 1b).

Our main contributions are:

- We characterize a previously unidentified optimization problem in hypernetwork training, and show that it leads to large gradient variance and unstable training dynamics.
- We propose a solution: Magnitude Invariant Parametrizations (MIP), a hypernetwork formulation that addresses the issue without introducing additional training or inference costs.
- We rigorously study the proposed parametrization. We first compare it with the standard formulation and against popular normalization strategies, showing that it consistently leads to faster convergence and more stable training. We then extensively test it using various

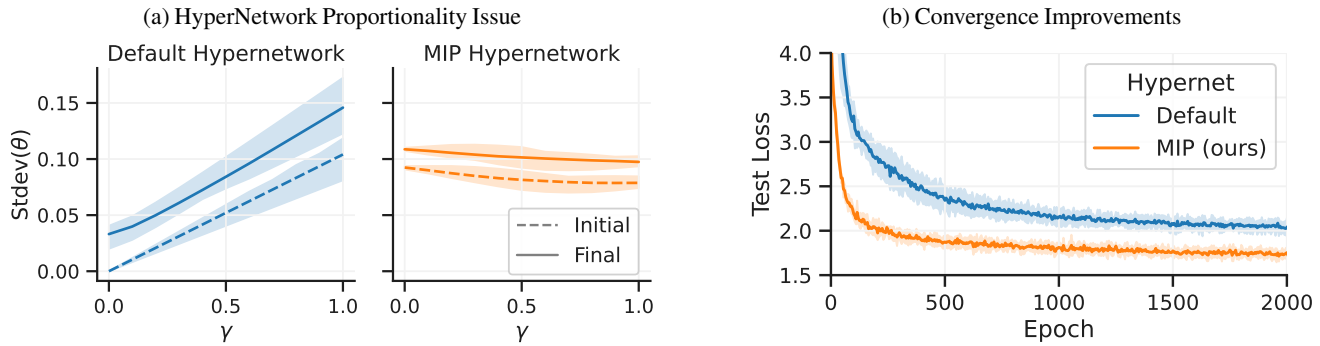


Figure 1: **(a) Proportionality Issue.** With *default* formulations, the scale of the predicted parameters θ (measured in standard deviation) is directly proportional to scale of the hypernetwork input γ at initialization (initial), and even after training the model (final). Our proposed Magnitude Invariant Parametrizations (MIP) mitigates this proportionality issue with respect to γ . **(b) Convergence Improvements.** Using MIP leads to faster convergence and result in reduced variance across network initializations than the default hypernetwork formulation.

choices of optimizer, input dimensionality, hypernetwork architecture, and activation function, finding that it improves hypernetwork training in all evaluated settings.

- We release our implementation as an open-source PyTorch library, HyperLight¹. HyperLight facilitates the development of hypernetwork models and provides principled choices for parametrizations and initializations, making hypernetwork adoption more accessible. We also provide code that enables using MIP seamlessly with existing models.

2. Related Work

Research into training stability and efficiency of neural networks involves a variety of strategies, including parameter initialization strategies, normalization techniques, and adaptive optimization.

Parameter Initialization. Deep neural networks experience unstable training dynamics in the presence of exploding or vanishing gradients [14]. Weight initialization plays a critical role in the magnitude of gradients, particularly during the early stages of training. Commonly, weight initialization strategies focus on preserving the magnitude of activations during the forward pass and maintaining the magnitude of gradients during the backward pass [13, 16]. Our work demonstrates that existing initialization strategies can be ineffective when applied to hypernetworks.

Normalization Techniques. Normalization techniques control the distribution of weights and activations, often leading to improvements in convergence by smoothing the loss surface [7, 23, 31, 48]. Batch normalization is widely used to normalize activations using minibatch statistics, and methods like layer or group normalization instead normalize

across features [2, 55, 59]. Other methods reparametrize the weights using weight-normalization strategies or using self-normalizing networks [26, 41, 47]. As we show in our experiments, these strategies fail to resolve the proportionality issue we study. They either maintain the proportionality relationship (as in batch normalization), or eliminate proportionality by rendering the predicted weights independent of the hypernetwork input (as in layer normalization), eliminating the utility of the hypernetwork itself.

Adaptive Optimization. High gradient variance can be detrimental to model convergence in stochastic gradient methods [24, 46]. Solutions to mitigate gradient variance encompass adaptive optimization techniques, which aim to decouple the effect of gradient direction and gradient magnitude by normalizing by a history of previous gradient magnitudes [25, 60]. Similarly, applying momentum reduces the instantaneous impact of stochastic gradients [36, 40] by using parameter updates based on an exponentially decaying average of past gradients. These strategies are implemented by many widely-used optimizers, such as Adam [5, 25]. Our experiments show that although adaptive optimizers like Adam enhance hypernetwork optimization, they do not address the root cause of the identified proportionality issue, and most convergence problems still persist.

Fourier Features. High-dimensional Fourier projections have been used in feature engineering [42] and for positional encodings in language modeling applications to account for both short and long range relationships [56, 51]. Additionally, implicit neural representation models benefit from sinusoidal representations [50, 52]. Our work also uses low dimensional Fourier projections. We demonstrate their use as a means to project hypernetwork inputs to a vector space with constant Euclidean norm, mitigating the training challenge.

Residual Forms. Residual and skip connections are

¹Source code at <https://github.com/JJGO/hyperlight>

widely used in deep learning models and often improve model training, particularly with increasing network depth [18, 19, 28, 56]. Building on this intuition, instead of the hypernetworks predicting the network parameters directly, our proposed hypernetworks predict parameter *changes*, mitigating part of the proportionality problem at hand.

3. The Hypernetwork Proportionality Problem

Preliminaries. Deep learning tasks most often involve a model $f(x; \theta) \rightarrow y$, with learnable parameters θ . In hierarchical models using hypernetworks, the parameters θ of the *primary network* f are predicted by a *hypernetwork* $h(\gamma; \omega) \rightarrow \theta$ based on an input vector γ . Instead of learning the parameters θ of the primary network f directly, only the learnable parameters ω of the hypernetwork h are optimized using backpropagation. The specific nature of the hypernetwork inputs γ varies across applications, but regularly corresponds to a low dimensional quantity that models properties of the learning task, and is often a simple scalar or embedding vector [3, 11, 22, 29, 38, 54, 58].

Assumptions. For our analysis we assume the following about the hypernetwork formulation: 1) The architecture is a series of fully connected layers of the form $\phi(Wx + b)$ where W are the parameters, b the biases and $\phi(x)$ the non-linear activation function; 2) The activation satisfies $\phi(x) = \max(\alpha x, 0) + \min(\beta x, 0)$ for some coefficients α and β . This encompasses common choices such as ReLU, LeakyReLU or PReLU; 3) Bias vectors b are initialized to zero. Existing hypernetworks satisfy these properties for the large majority of applications [8, 10, 11, 15, 29, 33, 38, 54, 57, 58].

Input-Output Proportionality. We demonstrate that under these widely-used settings, inputs and outputs of hypernetworks involve a proportionality relationship, and describe how this can impede hypernetwork training. We show that 1) at initialization, any intermediate feature vector $x^{(k)}$ at layer k will be proportional to the hypernetwork input γ , even under the presence of non-linear activation functions, and 2) this leads to large gradient magnitude fluctuations detrimental to optimization.

We first consider the case where $\gamma \in \mathbb{R}$ is a scalar value. Let $h(\gamma; \omega)$ use a fully connected architecture composed of a series of fully connected layers

$$\begin{aligned} h(\gamma; \omega) &= W^{(n)}x^{(n)} + b^{(n)} \\ x^{(k+1)} &= \phi(W^{(k)}x^{(k)} + b^{(k)}) \\ x^{(1)} &= \gamma \end{aligned} \quad (1)$$

where $x^{(k)}$ is the input vector of the k^{th} fully connected layer with learnable parameters $W^{(k)}$ and biases $b^{(k)}$. To prevent gradients from exploding or vanishing when chaining several layers, it is common to initialize the parameters $W^{(i)}$ and biases $b^{(i)}$ so that either the magnitude of the activations is approximately constant across layers in the forward pass

(known as *fan in*), or so that the magnitude of the gradients is constant across layers in the backward pass (known as *fan out*) [13, 16]. In both settings, the parameters $W^{(i)}$ are initialized using a zero mean Normal distribution and bias vectors $b^{(i)}$ are initialized to zero. If $\gamma > 0$, and $\phi(x)$ has the common form specified above, at initialization the i^{th} entry of vector $x^{(2)}$ is

$$x_i^{(2)} = \phi(W_i^{(1)}\gamma + b^{(1)}) = \gamma\phi(W_i^{(1)}) \propto \gamma, \quad (2)$$

since $b^{(1)} = 0$ and $\phi(W_i^{(1)})$ is independent of γ . Using induction, we assume that for layer k , $x_j^{(k)} \propto \gamma \forall j$, and show this property for layer $k+1$. The value of the i^{th} element of vector $x^{(k+1)}$ is

$$x_i^{(k+1)} = \phi\left(b_i^{(k)} + \sum_j W_{ij}^{(k)}x_j^{(k)}\right) = \gamma\phi\left(\sum_j W_{ij}^{(k)}\alpha_j^{(k)}\right) \propto \gamma, \quad (3)$$

since $b_i^{(k)} = 0$, and the term inside ϕ is independent of γ . If γ is not strictly positive, we can reach the same proportionality result, but with separate constants for the positive and the negative range. This dependency holds regardless of the number of layers and the number of neurons per hidden layer, and also holds when residual connections are employed. When γ is a vector input, we find a similar relationship with the overall magnitude of the input and the magnitude of the output. Given the absence of bias terms, and the lack of multiplicative interactions in the architecture, the fully connected network propagates magnitude changes in the input. We provide further details in the supplementary material.

Training implications. Since $\theta = x^{(n+1)}$, this result leads to a proportionality relationship for the magnitude of the predicted parameters $\|\theta\|_2 \propto \|\gamma\|$ and their variance $\text{Var}(\theta) \propto \|\gamma\|^2$. As the scale of the primary network parameters θ will depend on γ , this will affect the scale of the layer outputs and gradients of the primary network. In turn, these large gradient magnitude fluctuations lead to unstable training dynamics for stochastic gradient descent methods [13].

Further Considerations. Our analysis relies on biases being at zero, which only holds at initialization, and does not include normalization layers that are sometimes used. However, in our experiments, we find that biases remain near zero during early training, and hypernetworks with alternative choices of activation function, input dimensionality, or with normalization layers, still suffer from the identified issue and consistently benefit from our proposed parametrization (see Section 6).

4. Magnitude Invariant Parametrizations

To address the proportionality dependency, we make two straightforward changes to the typical hypernetwork formulation: 1) We introduce an encoding function that maps inputs into a constant-norm vector space, and 2) we treat hypernetwork predictions as additive *changes* to the main network parameters, rather than as the parameters themselves. These changes make the primary network weight distribution

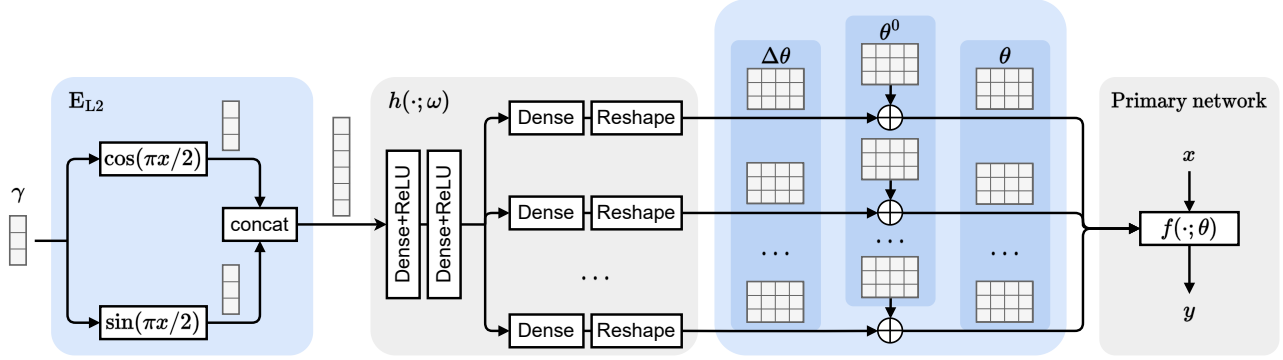


Figure 2: **Magnitude Invariant Parametrizations for Hypernetworks.** MIP first projects the hypernetwork inputs γ to a constant norm vector space. Then the outputs of the hypernetwork $\Delta\theta$ are treated as additive changes to a set of independent learnable parameters θ^0 to generate the primary network weights θ . In blue we highlight the main components of MIP, the input encoding E_{L2} and the residual formulation $\theta = \theta^0 + \Delta\theta$.

non-proportional to the hypernetwork input and stable across the range of hypernetwork inputs. Figure 2 illustrates these changes to the hypernetwork.

Input Encoding. To address the proportionality problem, we map the inputs $\gamma \in [0, 1]$ to a space with a constant Euclidean norm $\|E_{L2}(\gamma)\|_2 = 1$ using the function $E_{L2}(\gamma) = [\cos(\gamma\pi/2), \sin(\gamma\pi/2)]$. With this change, the input magnitude to the hypernetwork is constant $\|E_{L2}(\gamma)\| = 1 \forall \gamma$, so $\|x^{(1)}\| \not\propto \gamma$. For higher-dimensional inputs, we apply this transformation to each input individually, leading to an output vector with double the number of dimensions. This transformation results in an input representation with a constant norm, thereby eliminating the proportionality effect.

For our input encoding we first map each dimension of the input vector to the range $[0, 1]$ to maximize output range of E_{L2} . We use min-max scaling of the input: $\gamma' = (\gamma - \gamma_{\min}) / (\gamma_{\max} - \gamma_{\min})$. For unconstrained inputs such as Gaussian variables, we first apply the logistic function $\sigma(x) = 1 / (1 + \exp(-x))$. If inputs span several orders of magnitude, we take the log before the min-max scaling as in [3, 11].

Output Encoding. Residual forms have become a cornerstone in contemporary deep learning architectures [18, 28, 56]. Motivated by these methods, we replace the typical hypernetwork framework with one that learns primary network f parameters (what is typically learned in existing formulations), and then uses the hypernetwork predictions as *additive* changes to these parameters. We introduce a set of learnable parameters θ^0 , and compute the primary network parameters as $\theta = \theta^0 + h(E_{L2}(\gamma); \omega)$.

This output additive encoding predicts weights that are independent of the input by decomposing the hypernetwork contribution as a combination of an independent term θ^0 and a dependent term $h(E_{L2}(\gamma); \omega)$. The output encoding also offers a straightforward and principled mechanism for initializing hypernetwork weights. First, the hypernetwork

weights ω can be initialized using common initialization methods for fully connected layers. Then, the independent parameters θ^0 can be initialized taking into consideration their role in the primary network.

Connection to Learned Embeddings. Our input encoding approach can be understood in relation to the encoding of categorical hyperparameters in hypernetworks. Commonly, embedding layers transform categorical inputs into learnable parameters [8, 15]. For a scalar input γ , the first fully connected layer’s weights, $W \in \mathbb{R}^{N \times 1}$, act similarly to a learned embedding vector e . For scalar inputs γ represented by magnitude, the traditional formulation scales this embedding vector linearly, $x^{(2)} = \gamma e$. In contrast, our input encoding method uses $W \in \mathbb{R}^{N \times 2}$, which can be decomposed into two embedding vectors, $W = \{e_0, e_1\}$. From this perspective, our encoding function can be viewed as interpolating between two learnable embeddings vectors, $x^{(2)} = \cos(\gamma\pi/2)e_0 + \sin(\gamma\pi/2)e_1$.

5. Experimental Setup

5.1. Tasks

We evaluate our proposed parametrization on several tasks involving hypernetwork-based models.

Bayesian Neural Networks. Hypernetwork models have been used to learn families of functions conditioned on a prior distribution [54]. During training, the prior representation $\gamma \in \mathbb{R}^d$ is sampled from the prior distribution $\gamma \sim p(\gamma)$ and used to condition the hypernetwork $h(\gamma; \omega) \rightarrow \theta$ to predict the parameters of the primary network model $f(x; \theta)$. Once trained, the family of posterior networks is then used to estimate parameter uncertainty or to improve model calibration. For illustrative purposes we first evaluate a setting where $f(x; \theta)$ is a feed-forward neural network used to classify the MNIST dataset. Then, we tackle a more

complex setting where $f(x; \theta)$ is a ResNet-like model trained the OxfordFlowers-102 dataset [37]. In both settings, we use the prior $\mathcal{N}(0, 1)$ for each input.

Hypermorph. Learning-based medical image registration networks $f(x_m, x_f; \theta) \rightarrow \phi$ register a moving image x_m to a fixed image x_f by predicting a flow or deformation field ϕ between them. The common (unsupervised) loss balances an image alignment term \mathcal{L}_{sim} and a spatial regularization (smoothness) term \mathcal{L}_{reg} . The learning objective is then $\mathcal{L} = (1 - \gamma)\mathcal{L}_{\text{sim}}(x_m \circ \phi, x_f) + \gamma\mathcal{L}_{\text{reg}}(\phi)$, where γ controls the trade-off. In Hypermorph [22], multiple regularization settings for medical image registration are learned jointly using hypernetworks. The hypernetwork is given the trade-off parameter γ as input, sampled stochastically from $\mathcal{U}(0, 1)$ during training. We follow the same experimental setup, using a U-Net architecture for the primary (registration) network and training with MSE for \mathcal{L}_{sim} and total variation for \mathcal{L}_{reg} . We train models on the OASIS dataset. For evaluation, we use the predicted flow field to warp anatomical segmentation label maps of the moving image, and measure the volume overlap to the fixed label maps [4].

Scale-Space Hypernetworks. We also use a hypernetwork to efficiently learn a family of models with varying internal rescaling factors in the downsampling and upsampling layers, as recently done in [38]. In this setting, γ corresponds to the *scale factor*. Given hypernetwork input γ , the hypernetwork $h(\gamma; \omega) \rightarrow \theta$ predicts the parameters of the primary network, which performs the spatial rescaling operations according to the value of γ . We study a setting where $f(x; \theta)$ is a convolutional network with variable resizing layers, the rescaling factor is sampled from $\mathcal{U}(0, 0.5)$, and evaluate using the OxfordFlowers-102 classification problem and the OASIS segmentation task.

5.2. Experiment Details

Model. We implement the hypernetwork as a neural network with fully connected layers and LeakyReLU activations [32] for all but the last layer, which has linear output. Hypernetwork weights are initialized using Kaiming initialization [17] on *fan out* mode and biases are initialized to zero. Unless specified otherwise, the hypernetwork architecture has two hidden layers with 16 and 128 neurons respectively. We use this implementation for both the default (existing) hypernetworks, and our proposed (MIP) hypernetworks.

Training. We use two popular choices of optimizer: SGD with Nesterov momentum, and Adam [36, 25]. We search over a range of initial learning rates and report the best performing models; further details are included in the Supplementary material A.

Implementation. An important contribution of our work is the release of HyperLight, our PyTorch hypernetwork framework. HyperLight not only implements our proposed hypernetwork parametrization but provides a modular and

composable API that facilitates the development of hypernetwork models. Using HyperLight, practitioners can employ existing non-hypernetwork model definitions and pretrained model weights, and can easily build models using hierarchical hypernetworks. HyperLight source code available at <https://github.com/JJGO/hyperlight>.

6. Experimental Results

6.1. Effect of Proportionality on Parameter and Gradient Distributions

First, we empirically show how the proportionality phenomenon affects the distribution of predicted weights θ and their corresponding gradients for the Bayesian neural networks on MNIST. Figures 3a and 3b compare the distributions of the primary network weights and layer outputs for a range of values of hypernetwork input γ . While the default hypernetwork parametrization is highly sensitive to changes in the input, the proposed MIP eliminates this dependency, with the resulting distribution closely matching that of the non-hypernetwork models. Furthermore, Figure 1a (in the introduction), shows that using the default formulation, the scale of the weights correlates linearly with the value of the hypernetwork input, and that, crucially, this correlation is still present after the training process ends. In contrast, MIP parametrizations lead to a weight distribution that is robust to the input γ , both at the start and end of training.

We also analyze how the proportionality affects the early phase of hypernetwork optimization by studying the distribution of gradient norms during training. Figure 3c shows the norm of the predicted parameter gradients $\|\nabla_{\theta} \mathcal{L}\|$ as training progresses. As our analysis predicted, hypernetworks with the default parametrization experience large swings in gradient magnitude because of the proportionality relationship between inputs and predicted parameters. In contrast, the MIP strategy leads to a substantially smaller variance and more stable gradient magnitude compared to the standard formulation.

6.2. Model Training Improvements

In this experiment, we analyze how MIP affects model convergence for the considered tasks. For all experiments, we found that MIP hypernetworks did not introduce a measurable impact in training runtime, so we report per-epoch steps.

Figure 4a shows the training loss and test accuracy for Bayesian networks trained on MNIST. We find that MIP parametrizations result in better loss and higher accuracy sooner during training. MIP also achieves substantially reduced variance across network initializations. Default parametrization suffers from sporadic training instabilities (spikes in the training loss), while MIP leads to stable training. We found similar results for models trained with SGD.

Figures 4b and 4c present convergence curves for the other two tasks. For Hypermorph, MIP parametrizations are crucial

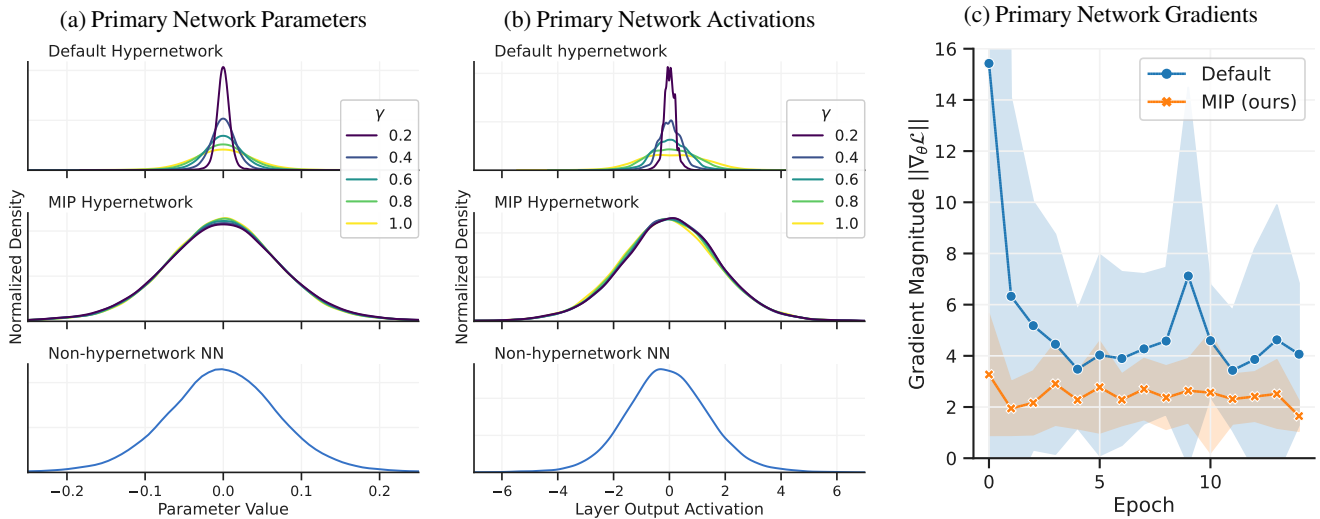


Figure 3: **Distributions of primary network parameters (a) and layer activations (b).** Measurements are taken at initialization for a default hypernetwork, our proposed MIP hypernetwork, and a conventional neural network with the same primary architecture. Distributions are shown as kernel density estimates (KDE) of the values due to the high degree of overlap between the distributions. In contrast, the MIP strategy leads to little change across input values and its distribution closely matches that of the non-hypernetwork model. **Evolution of Gradients (c)** Gradient magnitude with respect to hypernetwork outputs $\|\nabla_{\theta} \mathcal{L}\|$ during early training. Standard deviation is computed across minibatches in the same epoch. MIP leads to substantially smaller magnitude and improved robustness compared to the default parametrization.

when using SGD with momentum as otherwise the model fails to meaningfully train. For all choices of learning rate the default hypernetwork failed to converge, whereas with MIP parametrization it converged for a large range of values. With Adam, networks train meaningfully, and MIP models consistently achieve similar Dice scores substantially faster. They are less sensitive to weight initializations. While in this setting the Adam optimizer partially mitigates the gradient variance issue by normalizing by a history of previous gradients, the MIP parameterization leads to substantially faster convergence. Furthermore, for the Scale-Space segmentation, we find that for both optimizers MIP models achieve substantially faster convergence and better final accuracy compared to those with the default parametrization.

Comparison to normalization strategies. We compare the proposed parametrization to popular choices of normalization layers found in the deep learning literature. Using the default formulation, where the predicted weights start proportional to the hypernetwork input, we found that existing normalization strategies fall into two categories: they either keep the proportionality relationship present (such as batch normalization), or remove the proportionality by making the predicted weights independent of the hypernetwork input (such as layer or weight normalization). We provide further details in Section B of the supplemental material.

We test several normalization strategies. **BatchNorm-P**,

adding batch normalization layers to the primary network. **LayerNorm-P**, adding feature normalization layers to the primary network. **LayerNorm-H**, adding feature normalization layers to the hypernetwork layers. **WeightNorm**, performing weight normalization, which decouples the gradient magnitude and direction, to weights predicted by the hypernetwork [23, 2, 47]. Figure 5a shows the evolution of the test accuracy for the Scale-Space hypernetworks trained on OxfordFlowers. We report wall clock time, as some normalization strategies, such as BatchNorm, substantially increase the computation time required per iteration. For networks trained with SGD, normalization strategies enable training, but do not significantly improve on default hypernetworks when trained with Adam. Models trained with SGD momentum and hypernetwork feature normalization (LayerNorm-H) diverged early into training for all considered hyperparameter settings. Models trained with the proposed MIP parametrization lead to substantially faster convergence and better final model accuracy.

Ablation Analysis. We study the contribution of each of the two main components of the MIP parametrizations: input encoding and additive output formulation. Figure 5b shows the effect on convergence for two tasks. We found that both components reduce the proportionality dependency between the hypernetwork inputs and outputs, and that each component independently achieves substantial improvements in model convergence. However, we find that best results

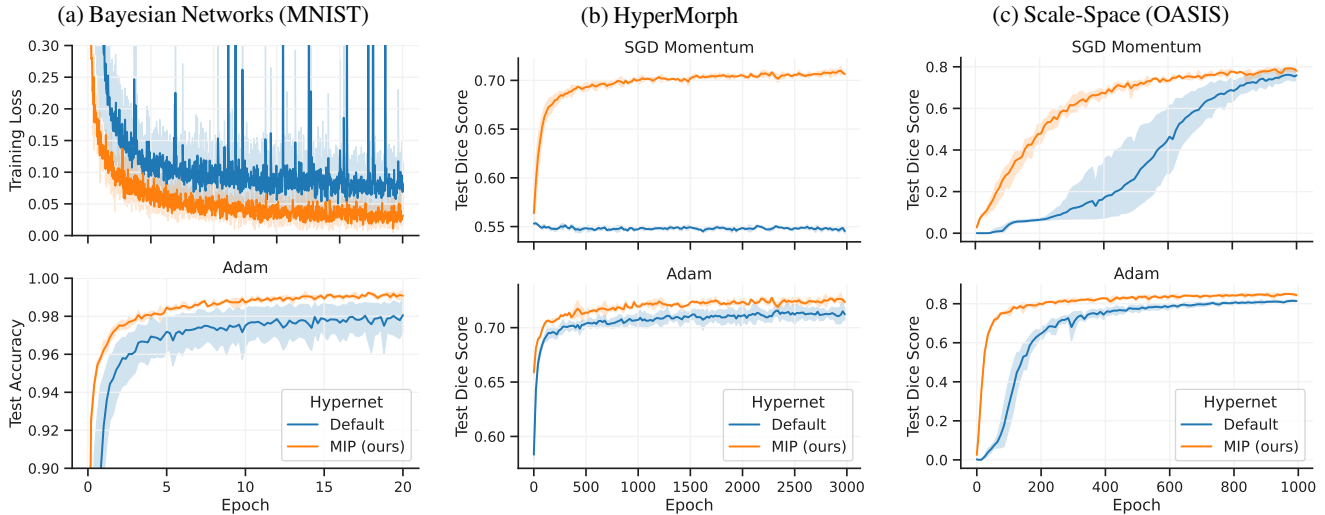


Figure 4: **Model Convergence Improvements.** Comparison between default hypernetworks and hypernetworks with MIP for the Bayesian networks on MNIST (a), HyperMorph (b) and Scale-Space hypernetworks trained on OASIS (c). In all cases, we find that the MIP parametrization leads to faster model convergence without any sacrifice in final model accuracy compared to the default parametrization. In (a) we observe that the default hypernetworks experience sporadic training instabilities (spikes in the training loss), whereas MIP hypernetworks present more stable training. In (b) and (c), we find that for default hypernetworks using the Adam optimizer substantially helps the training process, however, incorporating MIP leads to even better training dynamics.

(fastest convergence) are consistently achieved when both components are used jointly during training.

6.3. Robustness Analysis

Number of Input Dimensions to the Hypernetwork. We study the effect of the number of dimensions of the input to the hypernetwork model. We evaluate on the Bayesian neural network task, and we vary the number of dimensions of the input prior. We train models with geometrically increasing number of input dimensions, $\dim(\gamma) = 1, 2, \dots, 32$. Figure 5c shows that the proposed MIP strategy leads to improvements in model convergence and final model accuracy as we increase the dimension of the hypernetwork input γ .

Choice of Hypernetwork Architecture. We assess model performance when varying the properties of the hypernetwork architecture. We vary the width (number of hidden neurons per layer) and depth (number of layers)– fully connected networks with 3, 4 and 5 layers and with 16 and 128 neurons per layer, as well as an exponentially growing number of neurons per layer $\text{Dim}(x^n) = 16 \cdot 2^n$. We find that the MIP improvements generalize to the all tested hypernetwork architectures with analogous improvements in model training. We provide additional results in section B of the supplement.

Nonlinear Function Activation Ablation. While our method is motivated by the training instability present in hypernetworks with (Leaky)-ReLU nonlinear activation functions, we explored applying it to other common choices

of activation functions found in the literature: Tanh, GELU and SiLU [43, 20]. Figure 8 (in section B of the supplement) shows that MIP consistently helps for all choices of nonlinear activation function, and the improvements are similar to those of the LeakyReLU models.

7. Limitations

A limitation of this work is that all hypernetwork models used in our experiments are composed of fully connected layers and use activation and initialization choices commonly recommended in the literature. Similarly, we focused on two optimizers in our experiments, SGD with momentum and Adam. We believe that we would see similar results for other less common architectures and optimizers, but this remains an area of future work. Furthermore, we focus on training models from scratch. Given that hypernetworks are becoming increasingly popular in transfer learning tasks using pretrained models, we believe this will be an interesting avenue for future analysis of MIP.

8. Conclusion

We showed through analysis and experimentation that traditional hypernetwork formulations are susceptible to training instability, caused by the effect of the magnitude of hypernetwork input values on primary network weights and gradients, and that standard methods such as batch and layer normal-

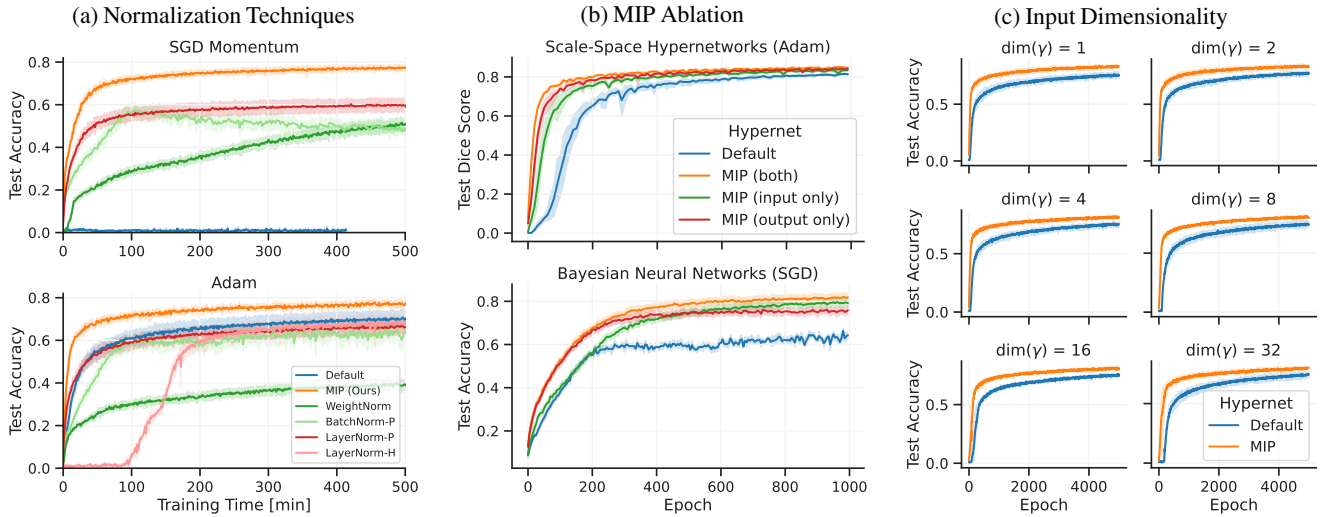


Figure 5: **(a) Normalization Strategies.** Comparison of hypernetworks trained with various normalization strategies for Scale-Space hypernetworks trained of OxfordFlowers-102. MIP provides substantially better results than the considered normalization strategies, achieving faster model convergence and better final test accuracy. **(b) Ablation Analysis.** Convergence results for separate components MIP on the Scale-Space Hypernetworks on OASIS using the Adam optimizer and the Bayesian networks trained with SGD on the OxfordFlowers-102 classification problem using SGD. Each component of the parametrization leads to improvements in final model accuracy as well as training convergence, and best results are achieved when using both components simultaneously. **(c) Input Dimensionality.** MIP parametrizations lead to clear improvements as we increase the dimensionality of the hypernetwork input γ for the Bayesian networks trained on OxfordFlowers-102.

ization do not solve the problem. We then proposed the use of a new method, Magnitude Invariant Parametrizations (MIP), for addressing this problem. Through extensive experiments, we demonstrated that MIP leads to substantial improvements in convergence times and model accuracy across multiple hypernetwork architectures, training scenarios, and tasks.

To further help with the adoption of hypernetworks, we release our hypernetwork learning library, HyperLight, which not only implements MIP but also provides a modular and composable API to facilitate the development of hypernetwork based models. Given that using MIP never reduces model performance and can dramatically improve training, we expect the method to be widely useful for training hypernetworks.

References

- [1] Yuval Alaluf, Omer Tov, Ron Mokady, Rinon Gal, and Amit Bermano. Hyperstyle: Stylegan inversion with hypernetworks for real image editing. In *Proceedings of the IEEE/CVF conference on computer vision and pattern recognition*, pages 18511–18521, 2022. 1
- [2] Jimmy Lei Ba, Jamie Ryan Kiros, and Geoffrey E Hinton. Layer normalization. *arXiv preprint arXiv:1607.06450*, 2016. 2, 6, 19
- [3] Juhan Bae, Michael R Zhang, Michael Ruan, Eric Wang, So Hasegawa, Jimmy Ba, and Roger Grosse. Multi-rate vae: Train once, get the full rate-distortion curve. *arXiv preprint arXiv:2212.03905*, 2022. 1, 3, 4
- [4] Guha Balakrishnan, Amy Zhao, Mert R Sabuncu, John Guttag, and Adrian V Dalca. Voxelmorph: a learning framework for deformable medical image registration. *IEEE transactions on medical imaging*, 38(8):1788–1800, 2019. 5
- [5] Lukas Balles and Philipp Hennig. Dissecting adam: The sign, magnitude and variance of stochastic gradients. In *International Conference on Machine Learning*, pages 404–413. PMLR, 2018. 2
- [6] Raphael Bensadoun, Shir Gur, Tomer Galanti, and Lior Wolf. Meta internal learning. *Advances in Neural Information Processing Systems*, 34:20645–20656, 2021. 1
- [7] Nils Bjorck, Carla P Gomes, Bart Selman, and Kilian Q Weinberger. Understanding batch normalization. *Advances in neural information processing systems*, 31, 2018. 2
- [8] Oscar Chang, Lampros Flokas, and Hod Lipson. Principled weight initialization for hypernetworks. In *International Conference on Learning Representations*, 2019. 3, 4

- [9] Lee R Dice. Measures of the amount of ecologic association between species. *Ecology*, 26(3):297–302, 1945. 12
- [10] Tan M Dinh, Anh Tuan Tran, Rang Nguyen, and Binh-Son Hua. Hyperinverter: Improving stylegan inversion via hypernetwork. In *Proceedings of the IEEE/CVF Conference on Computer Vision and Pattern Recognition*, pages 11389–11398, 2022. 1, 3
- [11] Alexey Dosovitskiy and Josip Djolonga. You only train once: Loss-conditional training of deep networks. In *International conference on learning representations*, 2020. 1, 3, 4
- [12] Benjamin Ehret, Christian Henning, Maria R. Cervera, Alexander Meulemans, Johannes von Oswald, and Benjamin F. Grewe. Continual learning in recurrent neural networks. In *International Conference on Learning Representations*, 2021. 1
- [13] Xavier Glorot and Yoshua Bengio. Understanding the difficulty of training deep feedforward neural networks. In *Proceedings of the thirteenth international conference on artificial intelligence and statistics*, pages 249–256. JMLR Workshop and Conference Proceedings, 2010. 2, 3
- [14] Ian Goodfellow, Yoshua Bengio, and Aaron Courville. *Deep learning*. MIT press, 2016. 2
- [15] David Ha, Andrew Dai, and Quoc V Le. Hypernetworks. *arXiv preprint arXiv:1609.09106*, 2016. 1, 3, 4
- [16] Kaiming He, Xiangyu Zhang, Shaoqing Ren, and Jian Sun. Delving deep into rectifiers: Surpassing human-level performance on imagenet classification. In *Proceedings of the IEEE international conference on computer vision*, pages 1026–1034, 2015. 2, 3
- [17] Kaiming He, Xiangyu Zhang, Shaoqing Ren, and Jian Sun. Delving deep into rectifiers: Surpassing human-level performance on imagenet classification. In *Proceedings of the IEEE international conference on computer vision*, pages 1026–1034, 2015. 5
- [18] Kaiming He, Xiangyu Zhang, Shaoqing Ren, and Jian Sun. Deep residual learning for image recognition. In *Proceedings of the IEEE conference on computer vision and pattern recognition*, pages 770–778, 2016. 3, 4
- [19] Kaiming He, Xiangyu Zhang, Shaoqing Ren, and Jian Sun. Identity mappings in deep residual networks. In *European conference on computer vision*, pages 630–645. Springer, 2016. 3
- [20] Dan Hendrycks and Kevin Gimpel. Gaussian error linear units (gelus). *arXiv preprint arXiv:1606.08415*, 2016. 7, 16
- [21] Christian Henning, Maria R. Cervera, Francesco D’Angelo, Johannes von Oswald, Regina Traber, Benjamin Ehret, Seijin Kobayashi, Benjamin F. Grewe, and João Sacramento. Posterior meta-replay for continual learning. In *Conference on Neural Information Processing Systems*, 2021. 1
- [22] Andrew Hoopes, Malte Hoffman, Douglas N. Greve, Bruce Fischl, John Guttag, and Adrian V. Dalca. Learning the effect of registration hyperparameters with hypermorph. *Machine Learning for Biomedical Imaging*, 1:1–30, 2022. 1, 3, 5, 12
- [23] Sergey Ioffe. Batch renormalization: Towards reducing minibatch dependence in batch-normalized models. *arXiv preprint arXiv:1702.03275*, 2017. 2, 6, 19
- [24] Rie Johnson and Tong Zhang. Accelerating stochastic gradient descent using predictive variance reduction. *Advances in neural information processing systems*, 26:315–323, 2013. 2
- [25] Diederik P Kingma and Jimmy Ba. Adam: A method for stochastic optimization. *arXiv preprint arXiv:1412.6980*, 2014. 2, 5
- [26] Günter Klambauer, Thomas Unterthiner, Andreas Mayr, and Sepp Hochreiter. Self-normalizing neural networks. In *Proceedings of the 31st international conference on neural information processing systems*, pages 972–981, 2017. 2
- [27] David Krueger, Chin-Wei Huang, Riashat Islam, Ryan Turner, Alexandre Lacoste, and Aaron Courville. Bayesian hypernetworks. *arXiv preprint arXiv:1710.04759*, 2017. 1
- [28] Hao Li, Zheng Xu, Gavin Taylor, Christoph Studer, and Tom Goldstein. Visualizing the loss landscape of neural nets. *Advances in neural information processing systems*, 31, 2018. 3, 4
- [29] Jonathan Lorraine and David Duvenaud. Stochastic hyperparameter optimization through hypernetworks. *arXiv preprint arXiv:1802.09419*, 2018. 3
- [30] Ilya Loshchilov and Frank Hutter. Fixing weight decay regularization in adam. *CoRR*, abs/1711.05101, 2017. 12
- [31] Ekdeep S Lubana, Robert Dick, and Hidenori Tanaka. Beyond batchnorm: Towards a unified understanding of normalization in deep learning. *Advances in Neural Information Processing Systems*, 34:4778–4791, 2021. 2
- [32] Andrew L Maas, Awni Y Hannun, and Andrew Y Ng. Rectifier nonlinearities improve neural network acoustic models. In *Proc. icml*, volume 30, page 3. Citeseer, 2013. 5
- [33] Matthew MacKay, Paul Vicol, Jon Lorraine, David Duvenaud, and Roger Grosse. Self-tuning networks: Bilevel optimization of hyperparameters using structured best-response functions. *arXiv preprint arXiv:1903.03088*, 2019. 3

- [34] Rabeeh Karimi Mahabadi, Sebastian Ruder, Mostafa Dehghani, and James Henderson. Parameter-efficient multi-task fine-tuning for transformers via shared hyper-networks. *arXiv preprint arXiv:2106.04489*, 2021. 1
- [35] Daniel S Marcus, Tracy H Wang, Jamie Parker, John G Csernansky, John C Morris, and Randy L Buckner. Open access series of imaging studies (oasis): cross-sectional mri data in young, middle aged, nondemented, and demented older adults. *Journal of cognitive neuroscience*, 19(9):1498–1507, 2007. 12
- [36] Yurii Nesterov. *Introductory lectures on convex optimization: A basic course*, volume 87. Springer Science & Business Media, 2013. 2, 5
- [37] M-E Nilsback and Andrew Zisserman. A visual vocabulary for flower classification. In *2006 IEEE Computer Society Conference on Computer Vision and Pattern Recognition (CVPR'06)*, volume 2, pages 1447–1454. IEEE, 2006. 5, 12
- [38] Jose Javier Gonzalez Ortiz, John Guttag, and Adrian V. Dalca. Amortized learning of dynamic feature scaling for image segmentation. *arXiv preprint arXiv:2304.05448*, 2023. 1, 3, 5, 13
- [39] Nick Pawlowski, Andrew Brock, Matthew CH Lee, Martin Rajchl, and Ben Glocker. Implicit weight uncertainty in neural networks. *arXiv preprint arXiv:1711.01297*, 2017. 1
- [40] Ning Qian. On the momentum term in gradient descent learning algorithms. *Neural networks*, 12(1):145–151, 1999. 2
- [41] Siyuan Qiao, Huiyu Wang, Chenxi Liu, Wei Shen, and Alan Yuille. Micro-batch training with batch-channel normalization and weight standardization. *arXiv preprint arXiv:1903.10520*, 2019. 2, 19
- [42] Ali Rahimi, Benjamin Recht, et al. Random features for large-scale kernel machines. In *NIPS*, volume 3, page 5. Citeseer, 2007. 2
- [43] Prajit Ramachandran, Barret Zoph, and Quoc V Le. Searching for activation functions. *arXiv preprint arXiv:1710.05941*, 2017. 7, 16
- [44] Neale Ratzlaff and Li Fuxin. Hypergan: A generative model for diverse, performant neural networks. In *International Conference on Machine Learning*, pages 5361–5369. PMLR, 2019. 1
- [45] Olaf Ronneberger, Philipp Fischer, and Thomas Brox. U-net: Convolutional networks for biomedical image segmentation. In *International Conference on Medical image computing and computer-assisted intervention*, pages 234–241. Springer, 2015. 12, 13
- [46] Nicolas Le Roux, Mark Schmidt, and Francis Bach. A stochastic gradient method with an exponential convergence rate for finite training sets. *arXiv preprint arXiv:1202.6258*, 2012. 2
- [47] Tim Salimans and Durk P Kingma. Weight normalization: A simple reparameterization to accelerate training of deep neural networks. *Advances in neural information processing systems*, 29:901–909, 2016. 2, 6
- [48] Shibani Santurkar, Dimitris Tsipras, Andrew Ilyas, and Aleksander Mądry. How does batch normalization help optimization? In *Proceedings of the 32nd international conference on neural information processing systems*, pages 2488–2498, 2018. 2
- [49] Joan Serrà, Santiago Pascual, and Carlos Segura. Blow: a single-scale hyperconditioned flow for non-parallel raw-audio voice conversion. *arXiv preprint arXiv:1906.00794*, 2019. 1
- [50] Vincent Sitzmann, Julien Martel, Alexander Bergman, David Lindell, and Gordon Wetzstein. Implicit neural representations with periodic activation functions. *Advances in Neural Information Processing Systems*, 33, 2020. 2
- [51] Jianlin Su, Yu Lu, Shengfeng Pan, Ahmed Murtadha, Bo Wen, and Yunfeng Liu. Roformer: Enhanced transformer with rotary position embedding. *arXiv preprint arXiv:2104.09864*, 2021. 2
- [52] Matthew Tancik, Pratul P Srinivasan, Ben Mildenhall, Sara Fridovich-Keil, Nithin Raghavan, Utkarsh Singhal, Ravi Ramamoorthi, Jonathan T Barron, and Ren Ng. Fourier features let networks learn high frequency functions in low dimensional domains. *arXiv preprint arXiv:2006.10739*, 2020. 2
- [53] Yi Tay, Zhe Zhao, Dara Bahri, Don Metzler, and Da-Cheng Juan. Hypergrid transformers: Towards a single model for multiple tasks. 2021. 1
- [54] Kenya Ukai, Takashi Matsubara, and Kuniaki Uehara. Hypernetwork-based implicit posterior estimation and model averaging of cnn. In *Asian Conference on Machine Learning*, pages 176–191. PMLR, 2018. 1, 3, 4
- [55] Dmitry Ulyanov, Andrea Vedaldi, and Victor Lempitsky. Instance normalization: The missing ingredient for fast stylization. *arXiv preprint arXiv:1607.08022*, 2016. 2, 19
- [56] Ashish Vaswani, Noam Shazeer, Niki Parmar, Jakob Uszkoreit, Llion Jones, Aidan N Gomez, Łukasz Kaiser, and Illia Polosukhin. Attention is all you need. *Advances in neural information processing systems*, 30, 2017. 2, 3, 4
- [57] Johannes von Oswald, Christian Henning, Benjamin F. Grewe, and João Sacramento. Continual learning with hypernetworks. In *International Conference on Learning Representations*, 2020. 1, 3

- [58] Alan Q Wang, Adrian V Dalca, and Mert R Sabuncu. Regularization-agnostic compressed sensing mri reconstruction with hypernetworks. *arXiv preprint arXiv:2101.02194*, 2021. 1, 3
- [59] Yuxin Wu and Kaiming He. Group normalization. In *Proceedings of the European conference on computer vision (ECCV)*, pages 3–19, 2018. 2
- [60] Matthew D Zeiler. Adadelata: an adaptive learning rate method. *arXiv preprint arXiv:1212.5701*, 2012. 2
- [61] Lvmin Zhang and Maneesh Agrawala. Adding conditional control to text-to-image diffusion models, 2023. 1
- [62] Dominic Zhao, Johannes von Oswald, Seijin Kobayashi, João Sacramento, and Benjamin F Grewe. Meta-learning via hypernetworks. 2020. 1
- [63] Allan Zhou, Tom Knowles, and Chelsea Finn. Meta-learning symmetries by reparameterization. *arXiv preprint arXiv:2007.02933*, 2020. 1

Appendix

A. Additional Experimental Details

A.1. Datasets

MNIST. We train models on the MNIST digit classification task. We use the official MNIST database of handwritten digits. The MNIST database of handwritten digits comprises a training set of 60,000 examples, and a test set of 10,000 examples. We use the official train-test split for training data, and further divide the training split into training and validation using a stratified 80%-20% split. We use the digit labels and consider the 10-way classification problem.

OxfordFlowers-102. We use the OxfordFlowers-102 dataset, a fine-grained vision classification dataset with 8,189 examples from 102 flower categories [37]. We utilize this dataset as it poses a non-trivial learning task that does not quickly converge, and allows us to better study learning dynamics. We use the official train-test split for training data, and further divide the training split into training and validation using a stratified 80%-20% split. We perform data augmentation by considering random square crops of between 25% and 100% of the original image area and resizing images to 256 by 256 pixels. Additionally, we perform random horizontal flips and color jitter (brightness 25%, contrast 50%, saturation 50%). For evaluation we take the central square crop of each image and resize to 256 by 256 pixels.

OASIS We use a version of the open-access OASIS Brains dataset [22, 35], a medical imaging dataset containing 414 MRI scans from separate individuals, comprised of skull-stripped and bias-corrected images that are resampled into an affinely-aligned, common template space. For each scan, segmentation labels for 24 brain substructures in a 2D coronal slice are available. We use 64%, 16% and 20% splits for training, validation and test.

A.2. Bayesian Neural Networks

Primary Network. For the MNIST task, we use a LeNet architecture variant that uses ReLU activations as they have become more prevalent in modern deep learning models. Moreover, we replace the first fully-connected layer with two convolutional layers of 32 and 64 features. We found this change did not impact test accuracy in non-hypernetwork models, but it lead to more stable initializations for the default hypernetworks.

For the OxfordFlowers-102 task, the primary network f features a ResNet-like architecture with five downsampling stages with (16, 32, 64, 128, 128) feature channels respectively. For experiments including normalization layers, such as BatchNorm and LayerNorm, the learnable affine parameters of the normalization layers are not predicted by the hypernetworks and are optimized like in regular neural networks via backpropagation.

Training. We train using a categorical cross entropy loss. For both optimizers we use learning rate $\eta = 3 \times 10^{-4}$. Nevertheless, we found consistent results with the ones we report using learning rates in the range $\eta = [10^{-4}, 3 \times 10^{-3}]$. We sample γ from the uniform distribution $\mathcal{U}[0,1]$.

Evaluation. For evaluation we use top-1 accuracy on the classification labels. In order to get a more fine-grained evolution of the test accuracy, we evaluate on test set at 0.25 epoch increments during training. We report results with five model replicas with different random seeds.

A.3. HyperMorph

HyperMorph, a learning based strategy for deformable image registration learns models with different loss functions in an amortized manner. In image registration, the γ hypernetwork input controls the trade-off between the reconstruction and regularization terms of the loss.

Primary Network. For our primary network f we use a U-Net architecture [45] with a convolutional encoder with five downsampling stages with two convolutional layers per stage of 32 channels each. Similarly, the convolutional decoder is composed of four stages with two convolutional layers per stage of 32 channels each. We found that models with more convolutional filters performed no better than the described architecture.

Training. We train using the setup described in HyperMorph [22] using mean squared error for the reconstruction loss and total variation for the regularization of the predicted flow field. For the Adam optimizer we use $\beta_1 = 0.9$ and $\beta_2 = 0.999$ with decoupled decay [30] and $\eta = 10^{-4}$, but we found that learning rates $[10^{-4}, 3 \times 10^{-3}]$ lead to similar convergence results. For SGD with momentum, we tested learning rates $\eta = \{3 \times 10^{-2}, 10^{-2}, 3 \times 10^{-3}, 10^{-3}, 3 \times 10^{-4}, 10^{-4}, 3 \times 10^{-5}, 10^{-5}\}$. In all cases the default hypernetwork formulation failed to meaningfully train. We train for 3000 epochs, and sample γ uniformly in the range $[0,1]$ like in the original work.

Evaluation. Like [22], we use segmentation labels as the main means of evaluation and use the predicted flow field to warp the segmentation label maps and measure the overlap to the ground truth using the Dice score [9], a popular metric for

measuring segmentation quality. Dice score quantifies the overlap between two regions, with a score of 1 indicating perfect overlap and 0 indicating no overlap. For multiple segmentation labels, we compute the overall Dice coefficient as the average of Dice coefficients for each label. We report results with five model replicas with different random seeds.

A.4. Scale-Space Hypernetworks

We evaluate on a task where the hypernetwork input γ controls architectural properties of the primary network. We use γ to determine the amount of downsampling in the pooling layers. Instead of using pooling layers that rescale by a fixed factor of two, we replace these operations by a fractional bilinear sampling operation that rescales the input by a factor of γ .

Primary Network. For classification tasks, our primary network f features a ResNet-like architecture with five downsampling stages with (16, 32, 64, 128, 128) feature channels respectively. For experiments including normalization layers, such as BatchNorm and LayerNorm, the learnable affine parameters of the normalization layers are not predicted by the hypernetworks and are optimized like in regular neural networks via backpropagation.

For segmentation tasks, we model the primary network f using a U-Net architecture [45] with a convolutional encoder with five downsampling stages with two convolutional layers per stage of 32 channels each. Similarly, the convolutional decoder is composed of four stages with two convolutional layers per stage of 32 channels each.

Training. We sample the hypernetwork input γ uniformly in the range $[0,0.5]$ where $\gamma = 0.5$ corresponds to downsampling by 2. We train the multi-class classification task using a categorical cross-entropy loss, and train with a weight decay factor of 10^{-3} , and with label smoothing the ground truth labels with a uniform distribution of amplitude $\epsilon = 0.1$. For the segmentation tasks we train using a cross-entropy loss and then finetune using a soft-Dice loss term, as in [38]. For both optimizers we use learning rate $\eta = 1 \times 10^{-4}$. Nevertheless, we found consistent results with the ones we report using learning rates in the range $\eta = [1 \times 10^{-4}, 3 \times 10^{-3}]$.

A.5. Implementation Details

Platform. The experiments were carried out using an internal machine with 8 V100 GPUs and under the following platform settings:

Table 1: Platform Settings

Package	Version
Python	3.9.7
PyTorch	1.11.0
torchvision	0.12.0
CUDA	11.3.1
cuDNN	8.2.0

Results for the main set of results discussed in the paper totaled 93.7 gpu-hours whereas results in the supplemental material required an additional 79.4 gpu-hours.

B. Additional Experimental Results

B.1. Choice of Hypernetwork Architecture

In this experiment we test whether increasing the choice of hypernetwork architecture size has an effect on the improvements achieved by incorporating Magnitude Invariant Parametrizations (MIP). We study varying the width (the number of neurons per hidden layer) and the depth (the number of hidden layers) independently as well as jointly. For the depth, we consider networks with 3, 4 and 5 layers. For with, we consider having 16 neurons per layer, 128 neurons per layer, or having an exponentially growing number of neurons per layer (exp), following the expression $\text{Dim}(x^n) = 16 \cdot 2^n$.

We compare training networks using the default hypernetwork parametrization and MIP in the HyperMorph task. Figure 6 shows convergence curves for the evaluated settings, for several random initializations. Additionally, Figure 7 shows the distribution of final model performances for the range of inputs $\gamma \in [0, 1]$. We find that MIP models converge faster without sacrificing final model accuracy.

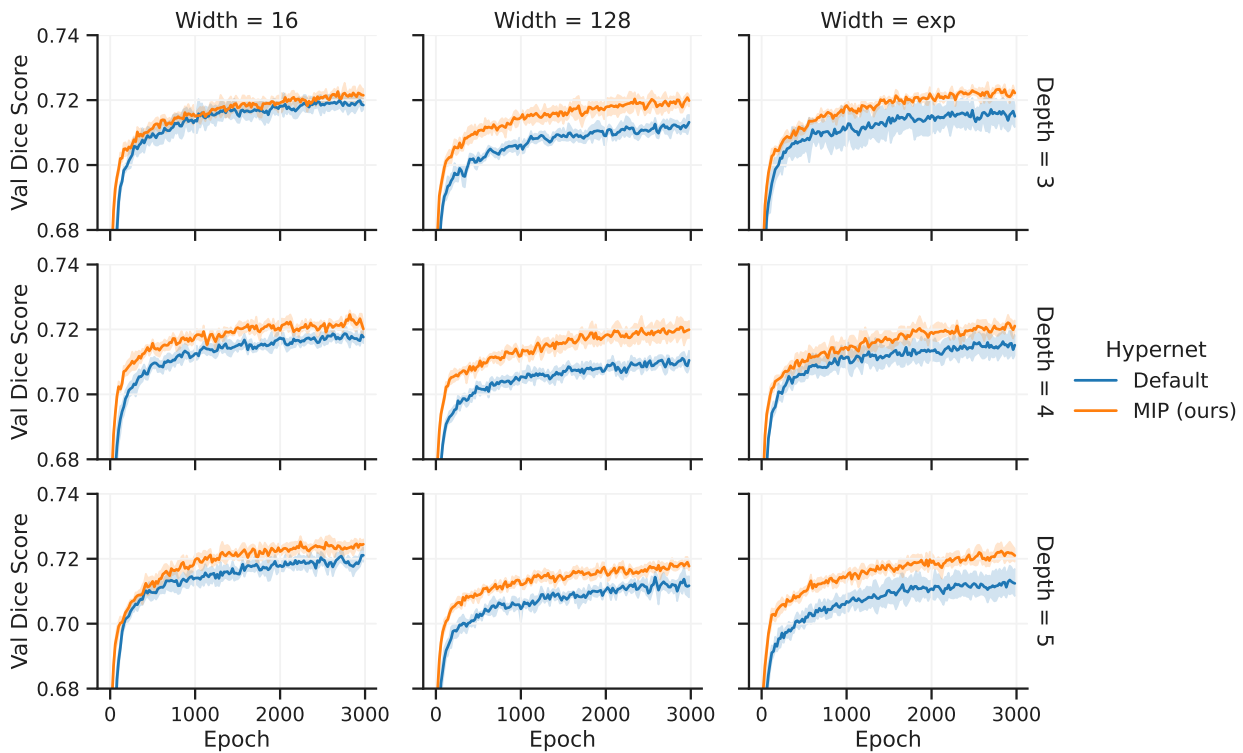


Figure 6: Model convergence for several configurations of depth and width of the hypernetwork architecture for default and MIP hypernetworks. Results correspond to HyperMorph on OASIS. Shaded regions measure standard deviation across hypernetwork initializations.

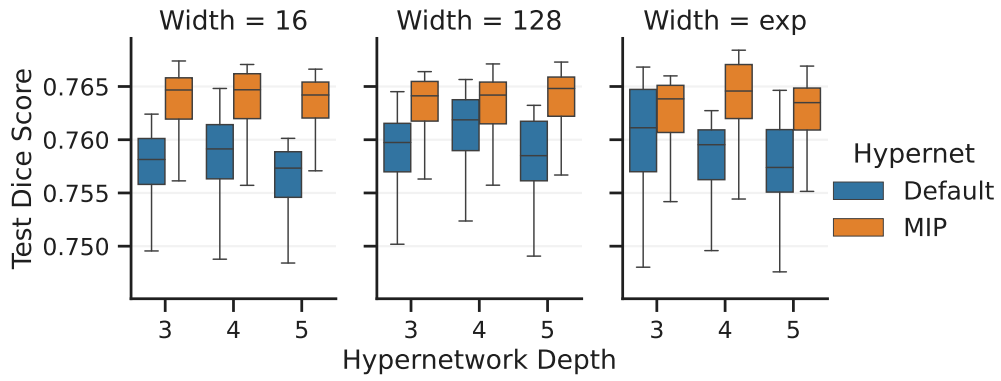


Figure 7: Test dice score for several configurations of depth and width of the hypernetwork architecture for default and MIP hypernetworks. Results correspond to HyperMorph on OASIS. Box-plots are reported over the range of hypernetwork inputs γ . For all hypernetwork architectures, MIP parametrizations consistently lead to more accurate models.

B.2. Choice of Nonlinear Activation Function

While our method is motivated by the training instability present in hypernetworks with (Leaky)-ReLU nonlinear activation functions, we explored applying it to other popular choices of activation functions. Moreover, some popular activation functions such as GELU or SiLU (also known as Swish) are close to the ReLU formulation [20, 43] We explore three alternative choices of nonlinear activations: Tanh, GELU and SiLU.

We evaluate on the Bayesian hypernetworks task on the OxfordFlowers-102 dataset with a primary convolutional network trained optimized with Adam. Figure 8 shows the convergence curves for Bayesian hypernetworks with a primary convolutional network trained on the OxfordFlowers classification task optimized with Adam. We see that MIP consistently helps for all choices of nonlinear activation function, and the improvements are similar to those of the LeakyReLU models.

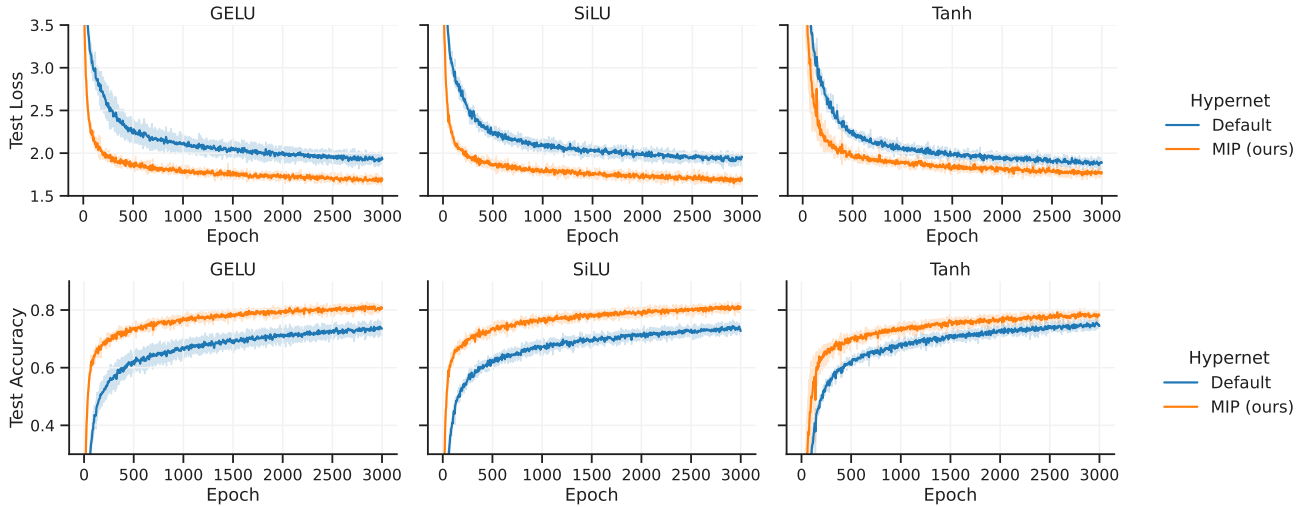


Figure 8: **MIP on alternative nonlinear activation functions** Test loss (top row) and test accuracy (bottom row) for bayesian hypernetworks trained on the OxfordFlowers classification task for various choices of nonlinear activation function in the hypernetwork architecture: GELU, SiLU and Tanh. For each setting, we train 3 independent replicas with different random initialization and report the mean (solid line) and the standard deviation (shaded region). We see significant improvements in model training convergence when the hypernetwork uses the proposed MIP parametrization.

B.3. Number of Input Dimensions

In this experiment, we study the effect of the number of dimensions of the input to the hypernetwork model to the hypernetwork training process, both for the default parametrization and for our MIP parametrization. We evaluate using the Bayesian Hypernetworks, as we can vary the number of dimensions of the input prior without having to define new tasks. We train models with geometrically increasing number of input dimensions, $\dim(\gamma) = 1, 2, \dots, 32$. We apply the input encoding to each dimension independently. We study two types of input distribution: uniform $\mathcal{U}(0,1)$ and Normal $\mathcal{N}(0,1)$ distributions. For MIP, we apply a sigmoid to the Normal inputs to constrain them to the $[0,1]$ range as specified by our method. We evaluate on the Bayesian hypernetworks task on the OxfordFlowers-102 dataset with a primary convolutional network optimized with Adam.

Figure 9 shows the convergence curves during training. Results indicate that the proposed MIP parametrization leads to improvements in model convergence and final model accuracy for all number of input dimensions to the hypernetwork and for both choices of input distribution. Moreover, we observe that the gap between MIP and the default parametrization does not diminish as the number of input dimensions grows.

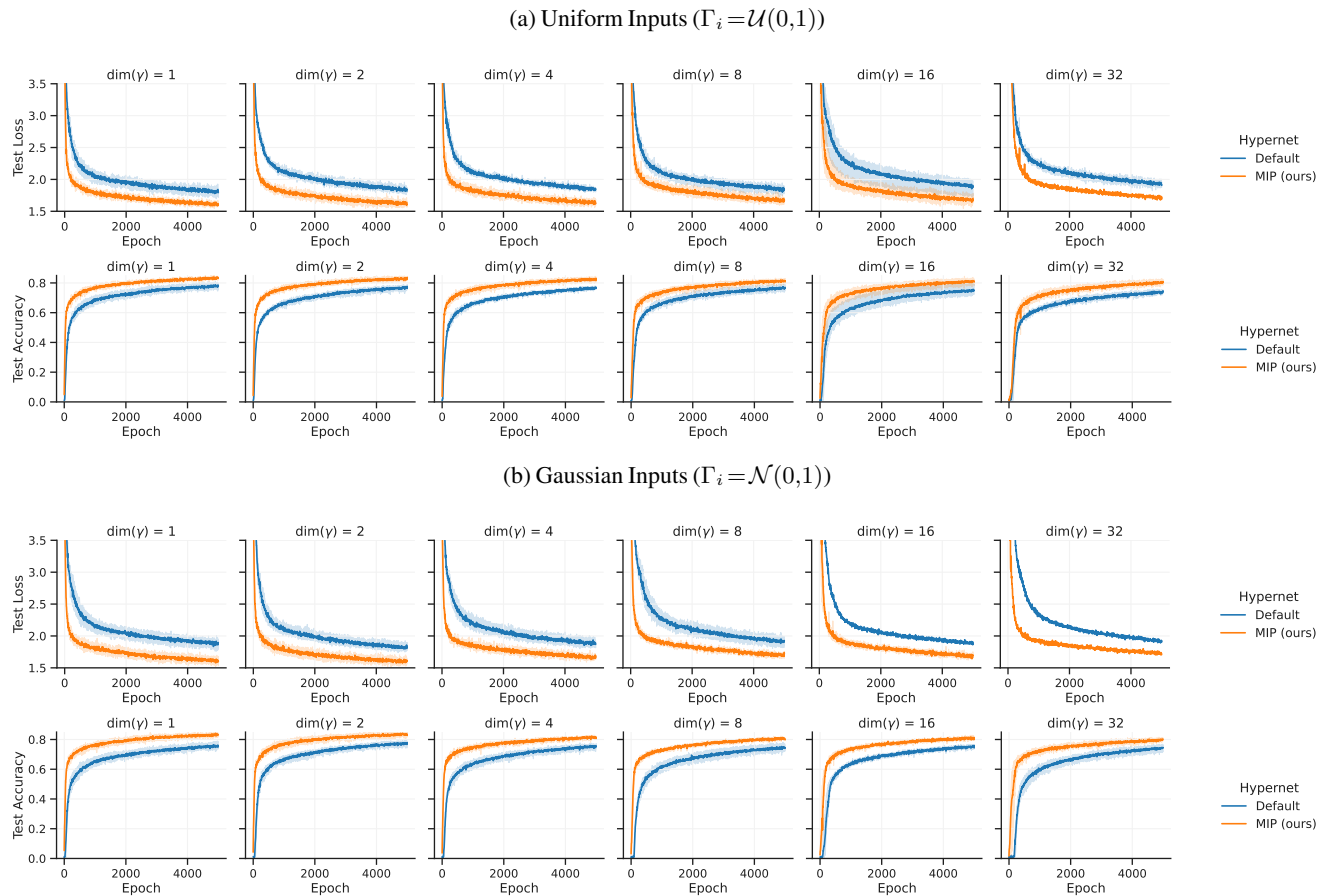


Figure 9: **Number of dimensions of hypernetwork input.** Test loss (top row) and test accuracy (bottom row) for Bayesian hypernetworks trained on the OxfordFlowers classification task for increasing number of dimensions of the hypernetwork input γ . We report results for different prior input distributions: Uniform (a) and Gaussian (b). For each setting, we train 3 independent replicas with different random initialization and report the mean (solid line) and the standard deviation (shaded region). We see significant improvements in model training convergence when the hypernetwork uses the proposed MIP parametrization.

B.4. Final Model Performance

Table 2: Final model results on the test set for the considered tasks and models. We report the average performance averaged across the range of γ inputs. We find MIP does not decrease model performance in any setting, while providing substantial improvements in several of them, specially when using the SGD optimizer. Standard Deviation across random initializations is included in parentheses.

Task	Data	Adam		SGD	
		Default	MIP	Default	MIP
Bayesian NN	MNIST	98.1 (1.1)	99.1 (0.3)	99.2 (0.2)	99.0 (0.2)
	OxfordFlowers-102	78.1 (1.9)	83.2 (0.3)	1.4 (0.1)	75.4 (0.5)
HyperMorph	OASIS	71.0 (0.3)	72.1 (0.3)	54.3 (0.4)	70.5 (0.2)
Scale-Space HN	OASIS	81.4 (0.3)	84.4 (0.6)	75.3 (2.7)	78.8 (1.4)

B.5. Normalization Strategies

Before developing MIP parametrizations we tested the viability of existing normalization strategies (such as Layer or Weight normalization) to deal with the identified proportionality phenomenon. While normalizing inputs and activations is a common practice in neural network training, hypernetworks present different challenges, and applying these techniques can actually be detrimental to the training process. Hypernetworks predict network parameters, and many of the assumptions behind parameter initialization and activation distribution do not easily translate between classical networks and hypernetworks.

An important distinction is that the main goal of our formulation is to ensure that the hypernetwork input has constant magnitude, not that is normalized (i.e. zero mean, unit variance). A normalized variable $z \sim \mathcal{N}(0,1)$ does not have constant magnitude (i.e. L2 norm), over its support, so normalization techniques do not solve the identified magnitude dependency and can actually lead to undesirable formulations. To show this, let $x \in \mathbb{R}^k$ be a hypernetwork activation vector, and $\gamma \in [0,1]$ the hypernetwork input. Then, according to the identified proportionality in Section 3.2, we know that $x = \gamma z$. Here x is the activation when the input is γ and z is a vector independent of γ . The normalization output will be

$$\text{Norm}(x) = \frac{x - \mathbb{E}[x]}{\text{Stdev}[x]} = \frac{\gamma z - \mathbb{E}[\gamma z]}{\text{Stdev}[\gamma z]} = \frac{\gamma z - \gamma \mathbb{E}[z]}{|\gamma| \text{Stdev}[z]} = \frac{z - \mathbb{E}[z]}{\text{Stdev}[z]},$$

making the output independent of the hypernetwork input γ . Following this reasoning, strategies like layer norm, instance norm or group norm in the hypernetwork will make the output of the model independent of the hypernetwork input, rendering the hypernetwork unusable for scalar inputs. For batch normalization cases it depends whether different hypernetwork inputs are used for each element in the minibatch. If not, the same logic applies as in the feature normalization strategies. Otherwise, the proportionality will still hold as the batch mean and standard deviation will be the same for all entries in the minibatch. Our experimental results confirm this. Hypernetworks with layer normalization fail to train in most settings. In contrast, we found consistently that training substantially improves when using our MIP formulation. See Figure 5a in the main body which shows that none of the tested normalization strategies is competitive with MIP in terms of model convergence or final model accuracy.

Batch Normalization - Applying batch normalization fails to deal with the proportionality phenomenon because it normalizes statistics that are independent of the magnitude of γ keeping the proportionality [23]. In our experiments batch normalization performed similar to the default formulation when included in either the hypernetwork or the primary network, failing to address the proportionality relationship. For instance, all of the results in Figure 9 use batch normalization layers as it is recommended in ResNet-like architectures. In this case, MIP still provides a substantial improvement in terms of model convergence and training stability.

Feature Normalization - Feature normalization techniques such as layer normalization, instance normalization or group normalization do remove the proportionality phenomenon we identify [2, 55]. However, by doing so they make the predicted weights independent of the input hyperparameter, limiting the modeling capacity of the hypernetwork architecture. Moreover, in our empirical analysis, networks with layer normalization in the hypernetwork layers failed to train entirely, with the loss diverging early in training.

Weight Normalization - We also considered techniques that decouple the gradient magnitude and direction such as weight normalization [41]. Performing weight normalization on the hypernetwork predictions effectively decouples the gradient magnitude and direction. We find that convergence is substantially lower compared to the default parametrization. Moreover, final model performance does not match the default parametrization.